Ultrasonics - Sonochemistry 63 (2020) 104934

Contents lists available at ScienceDirect

Ultrasonics - Sonochemistry

journal homepage: www.elsevier.com/locate/ultson

Assessment of the beneficial combination of electrochemical and ultrasonic activation of compounds originating from biomass

N. Neha[a], Md. H. Islam[b], S. Baranton[a], C. Coutanceau[a,*], B.G. Pollet[b,*]

[a] Catalysis and Non-Conventional Medium Group, IC2MP, UMR CNRS 7285, Université de Poitiers, 4 Rue Michel Brunet, 86022 Poitiers cedex, France
[b] Hydrogen Energy and Sonochemistry Research Group, Department of Energy and Process Engineering, Faculty of Engineering, Norwegian University of Science and Technology (NTNU), NO-7491 Trondheim, Norway

ARTICLE INFO

Keywords:
Glucose
Oxidation
Platinum
Ultrasound
Sonoelectrochemistry

ABSTRACT

The electro-oxidation of organic molecules at the anode with simultaneous generation of hydrogen at the cathode in electrosynthesis reactors is considered as a promising and efficient process for the co-production of hydrogen and bio-sourced value-added chemicals. In this study and for the first time, we investigated the electro-oxidation of glucose and methylglucoside in 0.1 mol L^{-1} NaOH on polycrystalline Pt (real surface area = 14.5 ± 0.5 cm^2, roughness ≈ 5) in the potential range [0; +1.20 V *vs. rhe*] under *silent* and ultrasonic (bath, 45 kHz, P_{acous} = 11.20 W) conditions. A series of linear sweep voltammograms, chronoamperograms and high-performance liquid chronoamperograms were generated. It was found that higher current densities were obtained under ultrasonic conditions over the potential range of +0.25 V to +1.10 V *vs. rhe*, indicating that higher oxidation rates were provided under ultrasonication. It was observed that the desorption of species from the Pt surface in the medium potential region was favoured, allowing free catalytic Pt sites for further adsorption and oxidation of reactants; and in the high potential region, high peak current densities in the presence of ultrasound was due to enhanced mass transport of the electroactive species from the bulk electrolyte to the Pt-polycrystalline electrode surface. HPLC studies confirmed that higher electrochemical activity was obtained in the presence of ultrasound than in the absence. In our conditions, it was also found that low frequency ultrasound did not change the selectivity of the glucose and methylglucoside electro-oxidation reactions but instead, a significant increase in the rate of conversion was observed.

1. Introduction

Owing to its huge abundance [1], renewable carbon from lignocellulosic biomass represents the best alternative for the future to fossil resources for both energy applications and platform chemicals for fine chemistry [2]. Cellulose, which is the main component of lignocellulosic biomass, can be depolymerized by various thermal treatments, or by using highly concentrated solutions of acids or bases [3]. However, cleaner processes have also been reported to yield glucose and glucose derivatives [4–6].

The oxidation products of glucose derivatives into carboxylic acids lead to the formation of important family of chemicals that can be used in various applications ranging from cosmetic and detergents (surfactants) to bio-sourced polymers [7]. Non-thermal activation methods, such as electrochemistry and sonochemistry (power ultrasound in chemistry), are known to increase the catalytic activity of biomass conversion [8–11].

On the one hand, electrocatalysis is a non-thermal activation method which appears to be increasingly interesting for the highly-efficient conversion of organic compounds containing multiple hydroxyl groups, e.g. polyols [12–14] and monosaccharides [10,11]. In addition, the electrooxidation of organic molecules at the anode of an electrosynthesis reactor occurs simultaneously with the production of hydrogen, which is considered as the most promising energy carrier for the future through its use in fuel cells, according to the following equation in the case of the electrochemical oxidation of glucose into gluconic acid:

$$C_6H_{12}O_6 + H_2O \rightarrow C_6H_{12}O_7 + H_2 \quad (1)$$

On the other hand, sonoelectrochemistry or the application of power ultrasound in electrochemistry offers many advantages, such as: a) enhanced electrochemical diffusion processes, b) increase in electrochemical rates and yields, c) increase in process efficiencies (electrode and current efficiencies), d) decrease in cell voltages and

* Corresponding authors.
E-mail addresses: christophe.coutanceau@univ-poitiers.fr (C. Coutanceau), bruno.g.pollet@ntnu.no (B.G. Pollet).

https://doi.org/10.1016/j.ultsonch.2019.104934
Received 13 November 2019; Received in revised form 14 December 2019; Accepted 17 December 2019
Available online 19 December 2019

electrode overpotentials, e) suppression of electrode fouling (and degassing at the electrode surface), f) improved electroplated and electrodeposited materials (in terms of quality, hardness, porosity and thickness), and g) improved electrode surface activation. Most of the observations are attributed to: a) electrode surface cleanliness, b) metal depassivation and gas bubble removal at the electrode surface, induced by acoustic cavitation and acoustic streaming, and c) enhanced mass-transport of electroactive species to the electrode surface (a thinning of the diffusion layer thickness, δ) [15–18].

It is then expected that the combination of power ultrasound and electrocatalysis (*sonoelectrocatalysis*) could enhance the efficiency for the activation and conversion of biomass issued compounds, such as glucose and methylglucoside, and hence the concomitant hydrogen evolution reaction (*her*). The objective of this work is to study the oxidation reactions of glucose and methylglucoside on a polycrystalline platinum electrode (Pt-poly, which is a reference material in electrocatalysis) in the absence and presence of low-frequency high-power ultrasound (45 kHz). Initially, oxidation reactions were studied by linear sweep voltammetry (LSV) to determine the activity of the Pt-poly electrode in aqueous alkaline medium, under silent and ultrasonic conditions. Then, analysis of the reaction products were performed by high performance liquid chromatography (HPLC) in order to study the effects of ultrasound on the selectivity. So far in the literature, many investigations have solely focussed on either using electrochemical or sonochemical/ultrasonic methods for the selective conversion of biomass, and from the authors' knowledge, no studies have been conducted to assess the use of power ultrasound for the electrochemical or sonoelectrochemical conversion of molecules from biomass.

2. Experimental methods

All electrochemical experiments were carried out using a potentiostat/galvanostat (Interface 5000E, Gamry Instruments) in a 3-electrode configuration. The sonoelectrochemical cell and setup was fully characterized by using the method of Pollet and co-workers [19,20] and placed in an *in-house* Faraday cage. This sonoelectrochemical (*SE*) cell ($\varnothing_{base} \sim 5$ cm, $A_{SE\ base} \sim 19.63$ cm^2) had a cooling jacket linked to a thermostated bath operating at preset temperatures and the electroanalyte ($V_e = 100$ mL) was placed in an inner cell. The temperature of the electroanalyte was measured with a Fluke 51 digital thermometer fitted to a K-type thermocouple. The working electrode (WE) is a polycrystalline platinum (Pt-poly) mesh of 3.06 cm^2 geometric surface area (*Ag*). The reference electrode (RE) was a home-made standard hydrogen electrode (*rhe*). The counter electrode (CE) was a Pt mesh. The distance between the ultrasonic bath transducers and the working electrode was ca. 10 cm. All working electrodes were electrochemically cleaned in sulfuric acid (1.0 mol L^{-1}) for 10 min prior to the experiments. They were then washed with ultrapure water (Millipore, 18.2 M Ω cm).

All chemical reagents were of AnalaR grade or equivalent. Aqueous solutions of 0.10 mol L^{-1} glucose (18.0 g L^{-1}) and methylglucoside (19.4 g L^{-1}) in 0.10 mol L^{-1} NaOH were prepared in High-quality Milli-Q water. All solutions were degassed by bubbling nitrogen (N_2) for 30 min prior to experiments. Ultrasound was provided a 45 kHz (*f*) ultrasonic bath (VWR, USC2600D, $P_{elec} \sim 50$ W, $P_{max,elec} \sim 300$ W @ 100% fixed amplitude). Fig. 1 displays the experimental set-up for the sonoelectrochemical experiments at 45 kHz.

The ultrasonic or acoustic powers were determined calorimetrically using the methods of Margulis et al. [21] and Contamine et al. [22] and using Eq. (2):

$$P_{acous} = (dT/dt)_{t=0} \times m \times C_p \quad (2)$$

where $(dT/dt)_{t=0}$ is the temperature slope of water per unit of ultrasonication time (at $t = 0$) in K s^{-1}; m is the mass of the water used in g and C_p is the specific heat capacity of water as 4.186 J g^{-1} K^{-1}. Here, the calorimetric method consists in measuring the heat dissipated in a volume of water, taking into account the water heat capacity (C_p) in which the acoustic energy is absorbed. This method assumes that all absorbed acoustic energy is transformed into heat. From the calorimetric experiments, four ultrasonic parameters can be determined: (i) the acoustic power, P_{acous} in W, (ii) the volumetric acoustic power, $P_{acous,vol}$ in W L^{-1}, (iii) the ultrasonic intensity, ψ corresponding to the ratio of the measured acoustic power, P_{acous} and the surface area of the electrochemical cell base in W cm^{-2} and the (iv) the acoustic efficiency $\varepsilon_{acous/elec}$ of dissipated ultrasonic or acoustic power P_{acous} to the electric power P_{elec} in %.

In our conditions, the acoustic power (P_{acous}), the volumetric acoustic power ($P_{acous,vol}$), the ultrasonic intensity (ψ) and the acoustic efficiency ($\varepsilon_{acous/elec}$) were found to be, 11.20 W, 112 W L^{-1}, 0.570 W cm^{-2} and 22.40% respectively.

Measuring the formation of radicals in an aqueous solution during ultrasonication is challenging due to the radical's short lifespan. There are several chemical dosimetry methods (e.g. terephthalic acid, Fricke and Weissler methods) for determining the hydrogen peroxide (H_2O_2) or hydroxyl radical (OH·) formation during ultrasonication. In this study, we used the Weissler dosimetry method, i.e. the ultrasonication of pure aqueous potassium iodide (KI) solution. 0.1 mol L^{-1} KI solution was ultrasonicated for 30 mins, as described by Iida et al. [23] and Son et al. [24] La Rochebrochard d'Auzay et al. [25] to determine OH· radical concentrations and the I_3^- formation was monitored by UV–visible spectrophotometry at a wavelength of 350 nm (λ_{max}) and using a molar absorptivity (ε) of 26,000 dm^3 mol^{-1} cm^{-1}.

Here, the reaction pathway is the direct oxidation of iodide ions I^- in solution by OH· forming iodine I (Eq. (3)).

$$OH\cdot + I^- \rightarrow OH^- + I \quad (3)$$

The iodine reacts with I^- to produce I_2^- (Eq. (4)) which subsequently give rises to I_2 (Eq. (5)).

$$I + I^- \rightarrow I_2^- \quad (4)$$

$$2I_2^- \rightarrow I_2 + 2I^- \quad (5)$$

Molecular iodine produced from these reaction pathways reacts with excess I^- to form triiodide ions, I_3^- (Eq. (6)).

$$I_2 + I^- \rightarrow I_3^- \quad (6)$$

The absorbance of I_3^- was then measured using a UV–VIS spectrometer.

This method also allows the determination of the rate of triiodide anion formation $\nu(I_3^-)$ (mol s^{-1}) and thus the rate of formation OH·, i.e. assuming that $\nu(I_3^-) = \nu(OH\cdot)$. Fig. 2 shows the $[I_3^-]$ *vs.* irradiation time and assuming linearity between $t = 10$ min and $t = 30$ min, the slope of the line gave $\nu(I_3^-)$ as ca. 6×10^{-4} μmol L^{-1} s^{-1} (6×10^{-10} mol L^{-1} s^{-1} or 6×10^{-11} mol s^{-1} for 0.1 L).

This finding is in good agreement with other studies for low-frequency high-power ultrasound [26].

High performance liquid chromatography (HPLC) were performed using a Knauer Azura HPLC equipped with a Transgenomic ICSep COREGEL 107H column for organic acids, aldehydes, alcohols and ketone molecules separation. Because no standard is available for the expected product from methylglucoside oxidation, the comparison of the HPLC peak positions is made with respect to those recorded with standards from glucose and xylose oxidation products at 0.10 M, neutralized with NaOH (when necessary): sodium gluconate, lithium xylonate, glucuronic, glucaric, formic, glycolic acids, and oxalic and glucaric diacids (purity ≥97%, except for lithium xylonate with purity ≥95%). Chromatography analyses are performed with 0.007 mol L^{-1} H_2SO_4 aqueous solution as eluent at 0.6 mL min^{-1} flow rate with a UV detector set at λ = 210 nm.

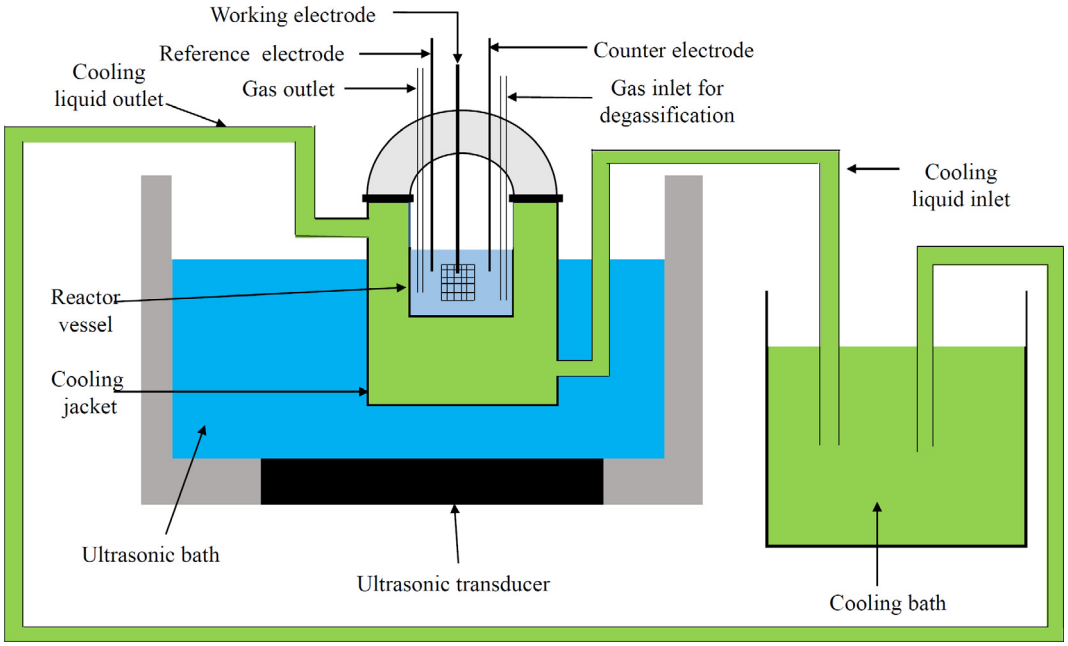

Fig. 1. Sonoelectrochemical setup using an ultrasonic bath (45 kHz).

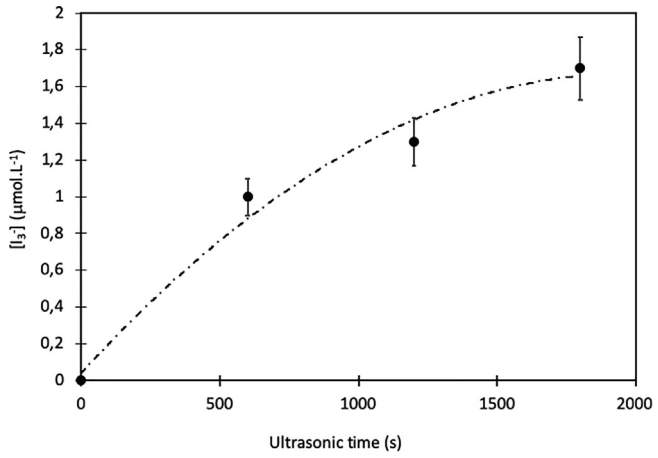

Fig. 2. Concentration of I_3^- *vs.* irradiation time for an ultrasonic bath operating at 45 kHz.

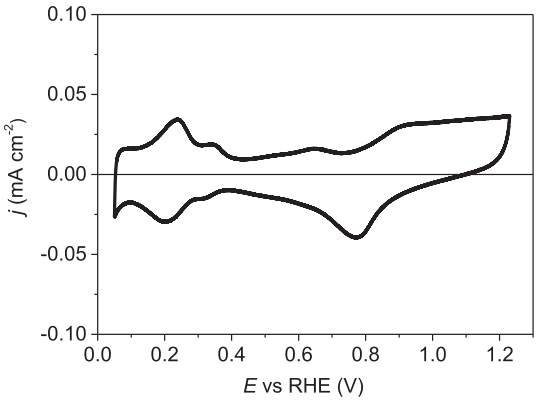

Fig. 3. Cyclic voltammogram recorded on the Pt-poly electrode in N_2-purged 0.1 mol L^{-1} NaOH (linear potential variation = 5 mV s^{-1}, N_2-purged electrolyte, T = 293 K).

3. Results and discussion

In this study, the reactions were investigated by cyclic and linear sweep voltammetry in presence of nitrogen on a bulk Pt polycrystalline electrode in order to determine the potential ranges where oxidation (positive current densities) and reduction (negative current densities) reactions occurred.

A complete CV of the background electrolyte (0.1 mol L^{-1} NaOH) was recorded on Pt-poly electrode in order to determine the real surface area (A_r) of the electrode, whereas LSVs were recorded in supporting electrolyte in presence of glucose and methylglucoside in order to check the electroreactivity of molecules.

Fig. 3 shows the complete CV of the Pt-poly electrode recorded for the background electrolyte in the absence of ultrasound. The shape of the voltammogram is typical of a platinum surface in alkaline media, with the redox feature in the +0.05 to +0.45 V *vs. rhe* corresponding to the underpotential adsorption of *H* (H_{upd}, negative current densities) and desorption of H_{upd} (positive current densities), the capacitive double layer in the +0.45 to +0.55 V *vs. rhe* range, and the Pt-OH then PtO formation (positive current densities) and reduction (negative current densities) in the +0.55 V to +1.25 V *vs. rhe* range. The real surface area (A_r) of the Pt-poly electrode can be calculated by determining, after correction from the capacitive current density, the coulombic charge associated to the H_{upd} desorption in the +0.05 to +0.45 V *vs. rhe*, potential region, according to (Eq. (7)) [27]:

$$A_r = \frac{\frac{1}{v}\int i(E)\mathrm{d}E}{Q_{monolayer}} \quad (7)$$

where $i(E)$ is the current (in µA) recorded at potential E (in V *vs. rhe*) in the hydrogen desorption region, v is the linear potential variation (in V s^{-1}) and $Q_{monolayer}$ is the t the coulombic charge related to the adsorption or desorption of a hydrogen monolayer on a polycrystalline Pt surface ($Q_{monolayer}$ = 210 µC cm^{-2}) [25,28,29].

A value of 14.5 ± 0.5 cm^2 for the real surface area was obtained against 3.06 cm^2 for the geometric surface area, e.g. a roughness ≈ 5.

Fig. 4(a) shows the LSVs of 0.10 mol L^{-1} glucose (18.0 g L^{-1}) in N_2-purged 0.10 mol L^{-1} NaOH background electrolyte in the absence (black line) and in the presence (red line) of ultrasonic irradiation. The LSV in the absence of ultrasound displays the typical three voltammetric features centered at ca. +0.25 V, +0.65 V and +1.10 V *vs. rhe*, typical of glucose oxidation on bulk Pt polycrystalline electrode [30]. It

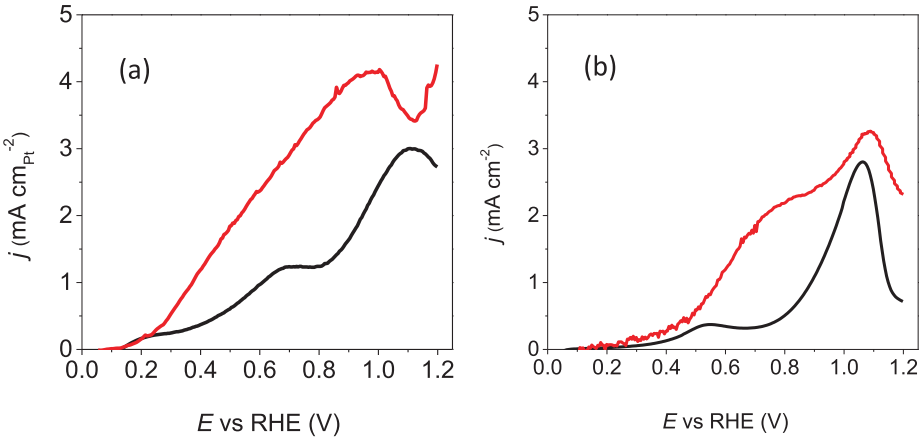

Fig. 4. Linear sweep voltammograms recorded on a Pt mesh of a real surface area of 14.5 ± 0.5 cm^2 in the absence (black line) and presence of 45 kHz ultrasound (red line) for (a) 0.1 mol L^{-1} glucose and (b) 0.1 mol L^{-1} methylglucoside in N_2-purged 0.1 mol L^{-1} NaOH (linear potential variation = 5 mV s^{-1}, N_2-purged electrolyte, T = 293 K).

can be noted that the onset potential of glucose electrooxidation does not change either in the absence or presence of ultrasound, remaining close to +0.12 V *vs. rhe*. However, ultrasonic activation starts to be effective for electrode potentials higher than ca. +0.25 V *vs. rhe*, and substantially higher current densities are observed under ultrasonic conditions over the potential range of +0.25 V to +1.10 V *vs. rhe*, indicating that higher oxidation rates are provided by ultrasound. For example, a ~1.4-fold increase in anodic peak current density is observed under ultrasonication ($j_{anodic\ peak}$ = +4.158 $mA.cm_{Pt}^{-2}$) when compared to *silent* conditions ($j_{anodic\ peak}$ = +3.002 $mA.cm_{Pt}^{-2}$). It is worth noting that a negative shift in anodic peak potential was observed under ultrasound, i.e. $\Delta E_{anodic\ peak} = E_{anodic\ peak,US} - E_{anodic\ peak,silent}$ = −125 mV. It is an interesting result, as similar findings were observed previously in other studies [15,31] For example, it was found that the shift in potential under ultrasound was caused by both the desorption of adsorbed species on the electrode surface and the continuous electrode surface cleaning. In the potential range of +0.12 V to +0.25 V *vs. rhe*, it is well-accepted that species from glucose strongly chemisorb on Pt-polycrystalline surface [28,32] are attributed to the first voltammetric peak. In the higher potential region, it is possible that the adsorbed gluconolactone on the Pt-poly surface is either oxidized chemically in presence of hydroxyl ions in the electrolyte or directly oxidized into gluconate. Other reactions involving C–C bond breaking and adsorbed CO species can also occur at low potentials, leading to CO_2 (CO_3^{2-}) and other degradation compounds at high potentials. These strongly adsorbed species in the low (+0.15 to +0.25 V *vs. rhe*) and medium (+0.25 to +0.80 V *vs. rhe*) potential regions limit the accessibility to Pt-poly surface. The observed high currents in the presence of ultrasound in the medium potential region indicate that the desorption of adsorbed species from the Pt surface is favoured, liberating free catalytic Pt sites for further adsorption and oxidation of glucose molecules. In the high potential region (+0.80 to +1.10 V *vs. rhe*), the high peak current in the presence of ultrasound may be due to enhanced mass transport of the electroactive species from the bulk electrolyte to Pt-polycrystalline electrode surface.

In the case of methylglucoside (Fig. 4(b)), a higher oxidation onset potential (ca. +0.25 V *vs. rhe*) and lower currents than in the case of glucose oxidation are achieved over the entire potential range employed. For example, a ~1.2-fold increase in anodic peak current density is observed under ultrasonication ($j_{anodic\ peak}$ = +3.262 $mA.cm_{Pt}^{-2}$) when compared to *silent* conditions ($j_{anodic\ peak}$ = +2.803 $mA.cm_{Pt}^{-2}$). However and contrarily to the sonoelectrooxidation of glucose, a positive shift in anodic peak potential was observed under ultrasound, i.e. $\Delta E_{anodic\ peak} = E_{anodic\ peak,US} - E_{anodic\ peak,silent}$ = +26 mV. These findings suggest that methylglucoside displays lower reactivity than glucose, owing to the protection of the anomeric group by a methyl group. Overall, similar trends under ultrasonic conditions are observable with methylglucoside as with glucose, and therefore similar conclusions can be drawn.

Chronoaperometry (CA) measurements were performed (not shown here) at constant potentials to accumulate the reaction products in order to perform HPLC analyses of the reaction medium in the absence and presence of ultrasound. Because methylglucoside is less electroreactive than glucose, the CA measurements were recorded at fixed potentials of +0.7 V *vs. rhe* for the methylglucoside conversion and +0.5 V *vs. rhe* for the glucose conversion, corresponding to approximately a current density of +0.4 mA cm^{-2} under ultrasonic irradiation in both cases (Fig. 4).

Fig. 5 shows a series of high-performance liquid chromatograms recorded after 4 h of CA in the absence (black line) and presence (red line) of ultrasound. In both cases, glucose oxidation (Fig. 5(a)) and methylglucoside oxidation (Fig. 5(b)), HPLC peaks exhibit higher intensity for the reaction mixture obtained under ultrasonic irradiation than under *silent* conditions. Increase in HPLC peaks intensity, and hence in peak surface area, is observed under ultrasonication compared to *silent* conditions. This observation confirms that higher electrochemical activity is obtained in the presence of ultrasound than in their absence.

Studying the HPLC peaks from the reaction products of glucose oxidation and comparing them to HPLC peaks of standards (Fig. 5(c)), the HPLC peaks could correspond: at ~6.1 min to the injection peak, at ~6.4 min to oxalic acid, at ~7.1 min to either glucaric, glucuronic or tartronic acids, at ~8.1 min to gluconic acid, at ~8.5 min to xylonic acid, at ~8.7 min to threonic acid, at ~9.4 min to glyceric acid, at ~10.7 min to glycolic acid and ~12.2 min to formic acid. The formation of gluconic, xylonic and threonic acids was already observed previously by Rafaïdeen et al. [11] after CA measurements on Pd_3Au_7/C electrode, whereas low C4 to C1 acids were also obtained by Parpot et al. [33,34] from electrolysis of hexose (mannose and galactose, isomers of glucose) on bulk platinum and gold electrodes.

Looking now at the HPLC peaks from methylglucoside oxidation (Fig. 5(b)), similar conclusions as for glucose can be drawn. However, in this case, the presence of gluconic, xylonic and threonic acids indicate that the anomeric function can be, in some extent, deprotected from the methyl group.

It is interesting to note that, in our conditions, hydroxy radicals do not seem to take part in the reactions as no obvious changes in the selectivity for the electrooxidation of either glucose or methylglucoside were observed. However, it can be speculated that OH· may be involved for electrode potentials higher than +0.25 V *vs. rhe*. At lower potentials, the adsorption on the Pt-poly surface is too “strong” to allow adsorbed species from glucose and methylglucoside to react with OH·, as shown in Fig. 4 with no observed activity enhancement; but for potentials higher than +0.25 V *vs. rhe*, the organic species’ adsorption affinity with the Pt surface is lowered, and adsorbed species can react with OH· and be desorbed as products, and this could explain the

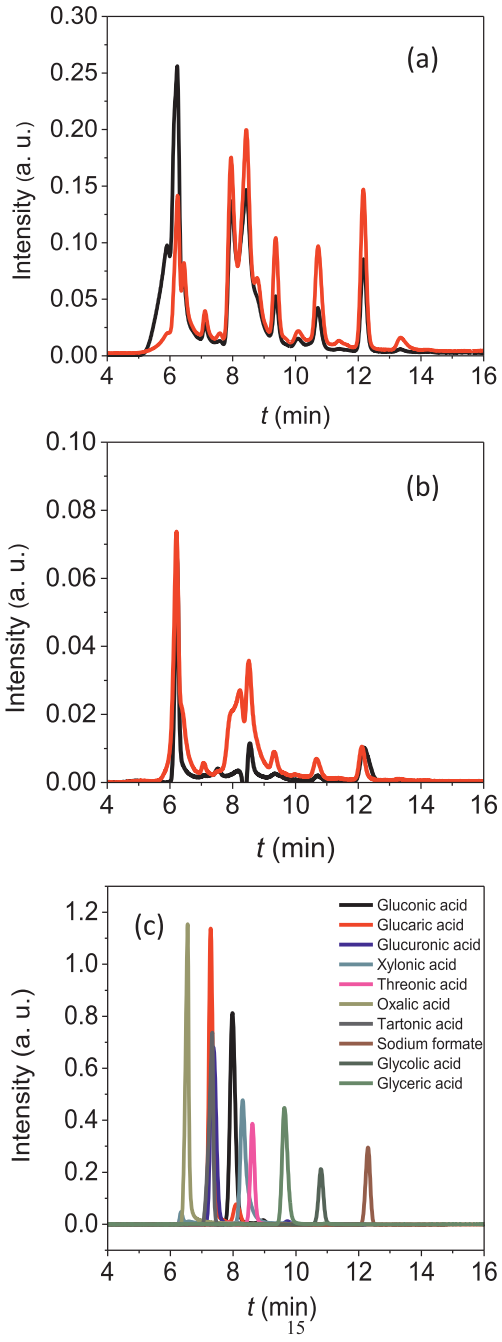

Fig. 5. High-performance liquid chromatograms recorded after 4 h of chronoamperometry (CA) measurements of (a) 0.1 mol L^{-1} glucose oxidation at +0.5 V *vs. rhe* in N_2 purged 0.1 mol L^{-1} NaOH aqueous solution and (b) 0.1 mol L^{-1} methylglucoside oxidation at +0.7 V *vs. rhe* in N_2 purged 0.1 mol L^{-1} NaOH aqueous solution in the absence (black line) and presence (red line) of ultrasound. (c) Chromatograms of standard solutions of expected reaction products at a fixed concentration of 0.1 mol L^{-1}.

higher activity in the medium potential region where mass transfer is not limiting.

This is an important observation since if the reaction rate is increased at the anode of an electrolysis cell, hydrogen production at the cathode will also be enhanced. This finding is in very good agreement with other studies. For example, and recently, Pollet et al. [35] showed that power ultrasound significantly increases the production of hydrogen caused by the lowering the so-called bubble overpotential (η_{bubble}) induced by electrode surface cleaning and mass transport enhancement.

Moreover, the increase in the concentration of degradation products yields an increase in the number of electrons exchanged (n), and in turn to an improved electrolysis cell efficiency at a given cell voltage. For example, the oxidation of glucose to gluconic acid involves the exchange of 2 electrons:

$$C_6H_{12}O_6 + H_2O \rightarrow C_6H_{12}O_7 + 2H^+ + 2e^- \quad (8)$$

whereas the formation of xylonic acid involves the exchange of 6 electrons:

$$C_6H_{12}O_6 + 2\,H_2O \rightarrow C_5H_{10}O_6 + CO_2 + 6H^+ + 6\,e^- \quad (9)$$

and that of lower molecular weight monoacids involves $(6 + 4n)$ electrons, with $1 \leq n \leq 4$, and for the complete oxidation into CO_2, 24 electrons are involved.

Thus, because the counter reaction consists of the proton (H^+) reduction reaction (hydrogen evolution reaction, *her*):

$$H^+ + 2\,e^- \rightarrow H_2 \quad (10)$$

the more C–C bond breaking is occurring, larger quantity of hydrogen evolved at lower cell voltages than the thermodynamic one for water electrolysis (+1.229 V *vs. rhe*) [36,37] can be achieved. This is of great industrial interest as most of the produced compounds, e.g. gluconic, xylonic, threonic, glyceric acids and glucaric diacids, are value added compounds [38,39,2]. Therefore, both these aspects could make sonoelectrochemical processes very interesting for the efficient co-production of hydrogen and bio-sourced value-added chemicals.

4. Conclusions

In this work, the electro-oxidation of glucose and methylglucoside in 0.10 mol L^{-1} NaOH on polycrystalline Pt under *silent* and ultrasonic conditions was investigated. Electrochemical and chromatography studies indicated that, in our experimental conditions, ultrasound enhances both the electrooxidation of glucose and methylglucoside i.e. an increase in the rate of conversion was significantly observed, but low frequency ultrasound (45 kHz) did not change the selectivity does not change the selectivity of the glucose and methylglucoside electro-oxidation reactions. The sonoelectro-oxidation of organic molecules at the anode with simultaneous generation of hydrogen at the cathode in electrosynthesis reactors is considered as a promising and efficient process for the co-production of hydrogen and bio-sourced value-added chemicals.

Declaration of Competing Interest

The authors declare that they have no known competing financial interests or personal relationships that could have appeared to influence the work reported in this paper.

Acknowledgements

The authors would like to thank the French AURORA program and the Research Council of Norway for financial support. The authors would also like to thank Lars Martin Ingebrigtsen and Henrik Erring Hansen of the *NTNU Hydrogen Energy and Sonochemistry Research group* for performing the dosimetry experiments. NN, CC and SB gratefully acknowledge the INCREASE Federation (FR CNRS 3707), the technogreen chair, the European Commission (FEDER) through the ECONAT project and the “Région Nouvelle Aquitaine”.

References

[1] M.A. Andrews, S.A. Laeren, G.L. Gould, in: G. Descotes, (Ed.), Carbohydrates as Organic Raw Materials II, VCH, Weinheim, Germany, 1993, pp. 3–27.
[2] C. Chatterjee, F. Pong, A. Sen, Chemical conversion pathways for carbohydrates,

Green Chem. 17 (2015) 40–71.
[3] I.M. O'Hara, Z. Zhang, W.O. Doherty, C.M. Fellows, in: R. Sanghi, V. Singh, (Eds.), Green Chemistry for Environmental Remediation, John Wiley & Sons, Inc., Salem (MA), USA, 2011, pp. 506–560.
[4] M. Benoit, A. Rodrigues, Q. Zhang, E. Fourré, K. De Oliveira Vigier, J.M. Tatibouët, F. Jérôme, Depolymerization of cellulose assisted by a nonthermal atmospheric plasma, Angew. Chem. Int. Ed. 50 (2011) 8964–8967.
[5] M. Benoit, A. Rodrigues, K. De Oliveira Vigier, E. Fourré, J. Barrault, J.M. Tatibouët, F. Jérôme, Combination of ball-milling and non-thermal atmospheric plasma as physical treatments for the saccharification of microcrystalline cellulose, Green Chem. 14 (2012) 2212–2215.
[6] Q. Zhang, M. Benoit, K. De Oliveira Vigier, J. Barrault, F. Jérôme, Pretreatment of microcrystalline cellulose by ultrasounds: effect of particle size in the heterogeneously-catalyzed hydrolysis of cellulose to glucose, Green Chem. 15 (2013) 963–969.
[7] T. Werpy, G. Petersen, A. Aden, J. Bozell, J. Holladay, J. White, A. Manheim, D. Elliot, L. Lasure, S. Jones, M. Gerber, K. Ibsen, L. Lumberg, S. Kelley. Pacific Northwest National Laboratory, National Renewable Energy Laboratory. Top Value-Added Chemicals from Biomass: Results of Screening for Potential Candidates from Sugars and Synthesis Gas. Department of Energy: Energy Efficiency and Renewable Energy, Oak Ridge, TN, 2004.
[8] G. Chatel, K. De Oliveira Vigier, F. Jérôme, Sonochemistry: what potential for conversion of lignocellulosic biomass into platform chemicals? ChemSusChem 7 (2014) 2774–2787.
[9] P.N. Amaniampong, Q.T. Trinh, K. De Oliveira Vigier, D.Q. Dao, N.H. Tran, Y. Wang, M.P. Sherburne, F. Jérôme, Synergistic effect of high-frequency ultrasound with cupric oxide catalyst resulting in a selectivity switch in glucose oxidation under argon, J. Am. Chem. Soc. 141 (2019) 14772–14779.
[10] S. Ghosh, Y. Holade, H. Remita, K. Servat, P. Beaunier, A. Hagège, K.B. Kokoh, T.W. Napporn, One-pot synthesis of reduced graphene oxide supported gold-based nanomaterials as robust nanocatalysts for glucose electrooxidation, Electrochim. Acta 212 (2016) 864–875.
[11] T. Rafaïdeen, S. Baranton, C. Coutanceau, Highly efficient and selective electrooxidation of glucose and xylose in alkaline medium at carbon supported alloyed PdAu nanocatalysts, Appl. Catal. B: Environ. 243 (2019) 641–656.
[12] A. Zalineeva, M. Padilla, U. Martinez, A. Serov, K. Artyushkova, S. Baranton, C. Coutanceau, P.B. Atanassov, Self-supported Pd-Bi catalysts for the electrooxidation of glycerol in alkaline media, J. Am. Chem. Soc. 136 (2014) 3937–3945.
[13] J. Cobos-Gonzalez, S. Baranton, C. Coutanceau, Development of Bi-modified PtPd nanocatalysts for the electrochemical reforming of polyols into hydrogen and value-added chemicals, ChemElectroChem 3 (2016) 1694–1704.
[14] M. Simões, S. Baranton, C. Coutanceau, Electrochemical valorization of glycerol, ChemSusChem 5 (2012) 2106–2124.
[15] B.G. Pollet, Power Ultrasound in Electrochemistry: From Versatile Laboratory Tool to Engineering Solution, John Wiley & Sons, Hoboken, NJ, USA, 2012.
[16] B.G. Pollet, A Short Introduction to Sonoelectrochemistry, Electrochem. Soc. Interface Fall 2008 (2018) 41–42.
[17] K. Yasui, in: B.G. Pollet, M. Ashokkumar (eds.), Acoustic Cavitation and Bubble Dynamics, Springer Briefs, 2018, ISBN: 978-3-319-68237-2.
[18] B.G. Pollet, M. Ashokkumar, in: B.G. Pollet, M. Ashokkumar (Eds.), Introduction to Ultrasound, Sonochemistry and Sonoelectrochemistry, SpringerBriefs, Berlin, Germany, 2019, ISBN: 978-3-030-25862-7.
[19] B.G. Pollet, J.-Y. Hihn, M.L. Doche, A. Mandroyan, J.P. Lorimer, T.J. Mason, Transport limited currents close to an ultrasonic horn: equivalent flow velocity determination, J. Electrochem. Soc. 154 (2007) E131–E138.
[20] J.Y. Hihn, M.L. Doche, A. Mandroyan, L. Hallez, B.G. Pollet, Respective contribution of cavitation and convective flow to local stirring in sonoreactors, Ultrason. Sonochem. 18 (2011) 881–887.
[21] M.A. Margulis, I.M. Margulis, Calorimetric method for measurement of acoustic power absorbed in a volume of a liquid, Ultrason. Sonochem. 10 (2003) 343–345.
[22] F. Contamine, A.M. Wilhelm, J. Berlan, H. Delmas, Power measurement in sonochemistry, Ultrason. Sonochem. 2 (1995) 43–47.
[23] Y. Iida, K. Yasui, T. Tuziuti, M. Sivakumar, Sonochemistry and its dosimetry, Microchem. J. 80 (2005) 159–164.
[24] Y. Son, M. Lim, M. Ashokkumar, J. Khim, Geometric optimization of sonoreactors for the enhancement of sonochemical activity, J. Phys. Chem. C 115 (2011) 4096–4103.
[25] S. La Rochebrochard d'Auzay, J.-F. Blais, E. Naffrechoux, Comparison of characterization methods in high frequency sonochemical reactors of differing configurations, Ultrason. Sonochem. 17 (2010) 547–554.
[26] L.M. Ingebrigtsen, Effects of ultrasonic frequency, acoustic power, and liquid height on radical production in a sonochemical reactor, Master's thesis in Energy and Environmental Engineering, Norwegian University of Science and Technology, 2019.
[27] C. Coutanceau, S. Baranton, T.W. Napporn, Platinum fuel cell nanoparticle syntheses: effect on morphology, structure and electrocatalytic behavior, in: A.A. Hashim (Ed.), The Delivery of Nanoparticles, Rijeka, InTech, 2012, pp. 403–431.
[28] T. Biegler, D.A.J. Rand, R. Woods, Limiting oxygen coverage on platinized platinum; relevance to determination of real platinum area by hydrogen adsorption, J. Electroanal. Chem. 29 (1971) 269–277.
[29] N.M. Markovic, B.N. Grgur, P.N. Ross, Temperature-dependent hydrogen electrochemistry on platinum low-index single-crystal surfaces in acid solutions, J. Phys. Chem. B 101 (1997) 5405–5413.
[30] B. Beden, F. Largeaud, K.B. Kokoh, C. Lamy, Fourier transform infrared reflectance spectroscopic investigation of the electrocatalytic oxidation of D-glucose: identification of reactive intermediates and reaction products, Electrochim. Acta 41 (1996) 701–709.
[31] B.G. Pollet, J.P. Lorimer, J.Y. Hihn, S.S. Phull, T.J. Mason, D.J. Walton, The effect of ultrasound upon the oxidation of thiosulphate on stainless steel and platinum electrodes, Ultrason. Sonochem. 9 (2002) 267–274.
[32] H.W. Lei, B. Wu, C.S. Cha, H. Kita, Electro-oxidation of glucose on platinum in alkaline solution and selective oxidation in the presence of additives, J. Electroanal. Chem. 382 (1995) 103–110.
[33] P. Parpot, N. Nunes, A.P. Bettencourt, Electrocatalytic oxidation of monosaccharides on gold electrode in alkaline medium: Structure–reactivity relationship, J. Electroanal. Chem. 596 (2006) 65–73.
[34] P. Parpot, P.R.B. Santos, A.P. Bettencourt, Electro-oxidation of d-mannose on platinum, gold and nickel electrodes in aqueous medium, J. Electroanal. Chem. 610 (2007) 154–162.
[35] Md Hujjatul Islam, M.T.Y. Paul, O.S. Burheim, B.G. Pollet, Recent developments in the sonoelectrochemical synthesis of nanomaterials, Ultrason. Sonochem. 59 (2019) 104711–104719.
[36] C. Lamy, T. Jaubert, Stève Baranton, C. Coutanceau, Clean hydrogen generation through the electrocatalytic oxidation of ethanol in a proton exchange membrane electrolysis cell (PEMEC): effect of the nature and structure of the catalytic anode, J. Power Sources 245 (2014) 927–936.
[37] C. Coutanceau, S. Baranton, Electrochemical conversion of alcohols for hydrogen production: a short overview, WIRE Energy Environ. (2016) 388–400.
[38] T. Werpy, G. Petersen, A. Aden, J. Bozell, J. Holladay, J. White, A. Manheim, D. Elliot, L. Lasure, S. Jones, M. Gerber, K. Ibsen, L. Lumberg, S. Kelley, Pacific Northwest National Laboratory, National Renewable Energy Laboratory. Top Value Added Chemicals from Biomass: Results of Screening for Potential Candidates from Sugars and Synthesis Gas, Department of Energy, Oak Ridge, TN, 2004.
[39] M. Simoes, S. Baranton, C. Coutanceau, Electrochemical valorization of glycerol, ChemSusChem 5 (2012) 2106–2124.